Kinetics and Thermodynamics of β2-Microglobulin Binding to the α3 Domain of Major Histocompatibility Complex Class I Heavy Chain†

Andrea M. Hebert,‡,§ Jason Strohmaier,‡,§ Mary C. Whitman,‡ Trina Chen,‡ Elena Gubina,‡ Dawn M. Hill,‡ Marc S. Lewis,|| and Steven Kozlowski*,‡

Division of Monoclonal Ab, Center for Biologics Evaluation and Research, Food and Drug Administration, and Molecular Interactions Resource, Division of Bioengineering and Physical Science, Office of Research Services, National Institutes of Health, Bethesda, Maryland 20892

Received October 16, 2000; Revised Manuscript Received January 30, 2001

ABSTRACT: The major histocompatibility complex (MHC) class I molecule plays a crucial role in cytotoxic lymphocyte function. Functional class I MHC exists as a heterotrimer consisting of the MHC class I heavy chain, an antigenic peptide fragment, and β2-microglobulin (β2m). β2m has been previously shown to play an important role in the folding of the MHC heavy chain without continued β2m association with the MHC complex. Therefore, β2m is both a structural component of the MHC complex and a chaperone-like molecule for MHC folding. In this study we provide data supporting a model in which the chaperone-like role of β2m is dependent on initial binding to only one of the two β2m interfaces with class 1 heavy chain. β2-Microglobulin binding to an isolated α3 domain of the class I MHC heavy chain accurately models the biochemistry and thermodynamics of β2m-driven refolding. Our results explain a 1000-fold discrepancy between β2m binding and refolding of MHC1. The biochemical study of the individual domains of complex molecules is an important strategy for understanding their dynamic structure and multiple functions.

The major histocompatibility complex class I (MHC1)[1] molecule and antigenic peptide are recognized by CD8+ cytotoxic T-lymphocytes (CTL) in CTL activation and lysis of targets (*1*). The heavy chain of the MHC class I molecule can interact noncovalently with a number of other molecules in the formation of a CTL activating complex. These include the MHC class I light chain or β2m, the antigenic peptide fragment, the T-cell receptor (TCR), and the CD8 molecule (*2*). The specificity of the CTL response resides in the selective MHC1 binding of specific antigenic peptide fragments and in the TCR recognition of these antigenic peptides and MHC1 (*3*, *4*). The MHC1 contact surface for TCR and peptide binding is formed by the α1 and α2 domains of the three-domain MHC class I heavy chain (*2*, *5*−*7*).

β2m, the nonpolymorphic component of the MHC1 complex, has been shown by X-ray crystallography to interact with the immunoglobulin-like α3 domain as well as the α1α2 domains of the MHC1 heavy chain (*8*). Mutations in the α1 (*9*, *10*) or α3 (*11*) domains of MHC1 lead to changes in β2m binding. These studies demonstrate that the functional interaction of the MHC1 heavy chain with β2m occurs at multiple surfaces on different domains.

In the absence of β2m, most MHC1 molecules are not expressed efficiently on the surface of cells (*12*, *13*). Although some MHC1 molecules, such as H-2L^d and H-2D^b, are transported to the cell surface without β2m, they have diminished levels of expression (*14*, *15*). This decreased MHC1 expression is not simply due to an export requirement for fully assembled MHC1 complexes. Transfection of β2m-negative cells with ER-retained β2m was able to salvage MHC1 cell surface expression (*16*). MHC1 folded in the presence of β2m was exported to the cell surface without bound β2m. A molecule, such as β2m, which promotes protein folding through a transient interaction fits the definition of a chaperone (*17*). Therefore, β2m plays two roles in MHC1: first, as a structural subunit of the assembled complex and, second, as a chaperone for the folding of the MHC1 heavy chain. A possible mechanism for β2m as a chaperone is facilitation of the interaction of MHC1 heavy chain with other chaperones, such as calreticulin, tapasin, TAP, and Erp57 (*18*, *19*). However, since β2m has been shown to promote stabilization or refolding of MHC1 on the cell surface in the absence of ER chaperones (*20*, *21*), it is likely that β2m also has a direct effect on MHC1 folding.

Although micromolar concentrations of high-affinity peptides can fold MHC1 in the absence of β2m, these same

† We thank the HHMI MCPS student intern program for their support.

* Correspondence should be addressed to: Steven Kozlowski DMA, CBER, FDA/8800 Rockville Pike, Bldg 29B-3NN08, HFM-561, Bethesda, MD-20892, USA. Tel: (301)-827-0719. Fax: (301)-827-0852. E-mail: Kozlowski @ CBER.FDA.GOV.

‡ Food and Drug Administration.

§ These authors contributed equally to this work.

|| National Institutes of Health.

[1] Abbreviations: MHC, major histocompatibility complex; MHC1, major histocompatibility class I molecules; CTL, cytotoxic T-lymphocyte; TCR, T-cell receptor; SPR, surface plasmon resonance; HBS-EP, HEPES-buffered saline with 3 mM EDTA and 0.005% polysorbate 20; hβ2m, human β2-microglobulin; mβ2m, murine β2-microglobulin; α3 par, H-2D^d α3 domain fusion protein; α3 227m, H-2D^d α3 domain fusion protein with a mutation at position 227.

10.1021/bi002392s
Published on Web 03/31/2001

peptides can stabilize MHC1 folded with β2m at significantly lower concentrations (*22*, *23*). Therefore, with physiologic concentrations of high-affinity peptides or any concentration of lower affinity peptides, β2m is limiting for the folding of MHC1 molecules.

The two roles of β2m, as structural subunit and chaperone, do not have the same dependence on β2m concentration. β2m binds to MHC1 heavy chain with an equilibrium dissociation constant (K_d) in the nanomolar range (*24*−*27*) while it refolds or stabilizes cell surface MHC1 at micromolar concentrations (*20*, *21*, *28*). We have previously demonstrated that human β2m (hβ2m) binds the isolated α3 domain of the MHC1 heavy chain with a K_d in the micromolar range (*29*). This suggested that β2m folding of the complete MHC1 heavy chain may be nucleated by a β2m−α3 interaction. Evidence with mutant cell lines (*30*) and assembly of newly translated molecules (*31*) suggest that the α3 domain is folded before the α1α2 domains and this folding can occur without β2m and peptide. The heavy chain α3 domain would then be available for initial binding of β2m, which would facilitate folding of the α1α2 domains of the heavy chain. The β2m-folded α1α2 domains would contribute to the heavy chain interaction with β2m and increase the likelihood of peptide binding in normal cells. Bound peptide would further stabilize the α1α2 domains of the heavy chain and increase the affinity of the folded MHC1 heavy chain for β2m to the nanomolar range.

To evaluate this model, we have further characterized the binding of β2m to α3 using surface plasmon resonance (SPR). We studied the binding of murine β2m (mβ2m) in addition to human β2m and determined the temperature dependence of the interaction. The species and temperature dependence of β2m binding to α3 and β2m refolding of MHC1 heavy chain are very similar. The chaperone-like effects of β2m can be explained by a β2m interaction with the α3 domain of a heavy chain with unfolded α1α2 domains.

EXPERIMENTAL PROCEDURES

α3 Domain Protein Expression and Purification. The H-2D^d α3 domain (α3 par) sequence was generated by PCR amplification of an H-D^d cDNA as described previously with the 5′ primer ACTCCATGGCAACAGATCCCCCAAAGGCCC and the 3′ primer GATGAATTCGACCCGGAAGGAGGAGGTTC (*29*). The α3 domain sequence was inserted between the *Nco*I and *Eco*RI sites of a modified pET21d vector (Novagen, Madison, WI). The vector was modified by ligating a synthetic oligonucleotide (GAGGAATTCTGGAATTTCGCAAGCTGTACATGCTGCACACGCTGAAATTAACGAAGCAGGAAGAGCACTCGAGCAC) between the *Eco*RI and *Xho*I sites of the pET21d bacterial expression vector. The completed construct was sequenced and found to be correct. The resulting construct, when transfected and induced, generated a 15 kDa fusion protein consisting of the H-D^d α3 domain fused to a vector-expressed sequence, a 17 amino acid peptide sequence from ovalbumin, and a polyhistidine tag.

Expression constructs were transfected into BL21(DE3) bacteria (Novagen, Madison, WI). Four hundred milliliter cultures of transfected bacteria in LB broth with 200 μg/mL carbenicillin (SIGMA, St. Louis, MO) were grown to an absorbance of 0.6 at 600 nm. The cultures were then induced with 1 mM IPTG (Sigma), and the cells were harvested by centrifugation after 3 h of induction at 37 °C or overnight induction at 28 °C. The bacteria were washed with PBS, and the pellet was frozen at −70 °C. The frozen pellet was thawed in 0.5 M NaCl/10 mM Tris, pH 8.0, with 1 mg/mL lysozyme (Sigma). After addition of imidazole (Sigma) to a concentration of 5 mM and Triton X-100 (Boehringer Mannheim, Indianapolis, IN) to a concentration of 1%, the samples were sonicated in a Brinkmann homogenizer (Brinkmann, Westbury, CT) for 3 × 30 s at a setting of 4. The homogenate was treated with ∼500 units of Benzonase (Sigma) in the presence of 5 mM MgCl. Inclusion bodies were pelleted by spinning at 15000*g*, and the soluble fraction was loaded onto buffer equilibrated NTA-Ni-resin (Qiagen, Santa Clarita, CA) for 1 h at 4 °C. The loaded NTA-Ni-resin was washed three times with 0.5 M NaCl/10mM Tris, pH 8.0/1% Triton X-100/5 mM imidazole buffer and then three times with 0.5 M NaCl/10 mM Tris, pH 8.0, buffer. The fusion protein was eluted with high-concentration imidazole (150−500 mM). In some cases, protein eluted with 150 mM imidazole was further purified by size exclusion chromatography. The eluted protein was dialyzed into HEPES-buffered saline (HBS) with 3 mM EDTA, and the protein concentration was measured by 280 nm absorbance. The extinction coefficient at 280 nm was calculated from the primary amino acid sequence. For experiments using the BIAcore, the buffer was adjusted with 10% polysorbate 20 (Biacore AB, Uppsala, Sweden) to 0.005% polysorbate 20 (HBS-EP buffer). For generation of the E227K mutant α3 domain (α3 227m), an H-D^d cDNA with the E227K mutation was used as the template for generating the mutant α3 insert. The completed construct was sequenced and purified in the same manner as the parental α3 construct.

β2m Expression and Purification. The recombinant human β2 microglobulin (hβ2m) and murine β2 microglobulin (mβ2m) were expressed using constructs in pET21d vectors generously supplied by Randall K. Ribaudo (*32*, *33*). The constructs were transfected into BL21(DE3) bacteria (Novagen). Cultures were grown at 37 °C to an absorbance of 0.8 at 600 nm and then induced with 1 mM IPTG for 2 h. The bacteria were harvested by centrifugation and washed and resuspended with 0.1 M Tris, pH 8.0, with 2 mM EDTA. Lysozyme (Sigma) was added at 0.5 mg/mL, and the bacteria were incubated overnight at 4 °C. Deoxycholate was added to a final concentration of 0.1%, and the mixture was sonicated on a Brinkmann homogenizer for 4 × 30 s. The inclusion bodies were pelleted by centrifugation at 15000*g*, and the soluble fraction was discarded. Inclusion bodies were washed three times with 0.1 M Tris, pH 8.0, with 2 mM EDTA and 0.1% deoxycholate followed by a wash with 0.1 M Tris, pH 8.0/2 mM EDTA. The pellet was resuspended with 10 mL of 6 M guanidine hydrochloride/0.1 mM DTT/0.1 M Tris, pH 8.0/2 mM EDTA. The dissolved protein was added to 1 L of prechilled 0.4 M arginine/0.1 M Tris/2 mM EDTA/5 mM reduced glutathione/0.5 mM oxidized glutathione and left in the cold room for a minimum of 3 days to refold. The protein was then diafiltered for 5 volume changes with HBS/3 mM EDTA and then concentrated using an Amicon ultrafiltration cell. The concentrated β2m was then purified by size exclusion chromatography. Both human and murine β2m were purified in the same manner.

Size Exclusion Chromatography. For β2m purification, 200 μL of protein was loaded onto a Superose 12 column (Pharmacia LKB) using the FPLC system (Pharmacia LKB) and run at 0.4 mL/min with HBS-EP buffer. For analysis and purification of α3 domain proteins, 200−500 μL of protein was loaded onto a Superdex 75 column (Pharmacia LKB) using the P-500 pump (Pharmacia LKB) at 0.5 mL/min with HBS-EP buffer. Half-milliliter fractions were collected, and protein concentration was determined by 280 nm absorbance. BSA (67 kDa), trypsinogen (24 kDa), and ribonuclease A (13.7 kDa) from Sigma were used as size standards.

Antibodies and Cell Lines. Anti-tetra-HIS antibody was purchased from Qiagen. Anti-H-2D^d conformationally dependent antibody (34.5.8S) was purchased from Pharmingen, San Diego, CA. The LKD8 cell line, a peptide transport deficient EE2H3 embryonic cell line transfected with H-2D^d (*34*), was the generous gift of David H. Margulies.

Flow Cytometry β2m MHC1 Folding Assay. Human and murine β2m were titrated at the indicated concentrations in 12-well tissue culture plates containing 1 mL of OPTI-MEM medium with 0.5% BSA and 0.5×10^6 LKD8 cells per well. After an overnight incubation at 26−28 °C, the cells were spun down at 4 °C. A half-microgram of the biotinylated anti-H-2D^d conformationally dependent antibody, 34.5.8S (Pharmingen), was added to the cells. Cells receiving no primary antibody served as controls. An experiment in which a biotinylated isotype matched antibody (Pharmingen) was used as a control gave similar results. After a 30 min incubation on ice, the cells were washed with 0.5% BSA/OPTI-MEM medium, and 50 μL of streptavidin−FITC (Pharmingen) diluted 1:50 in 0.5% BSA/OPTI-MEM was added to the cells for an additional 30 min incubation on ice. The cells were then washed with 3 mL 0.5% BSA/OPTI-MEM and analyzed on a FACScan Plus (Becton and Dickenson, Mountain View, CA) flow cytometer. Data analysis was performed using the Cell Quest software (Becton and Dickenson).

Surface Plasmon Resonance (SPR) Experiments and Data Analysis. All SPR experiments were performed on the BIAcore 3000 biosensor (Biacore AB). Anti-HIS antibody, diluted in 10 mM acetate buffer, pH 4.5, was covalently coupled to the carboxymethylated dextran matrix on a CM5 sensor chip (Biacore AB) by using the amine coupling kit as described (*35*). Experiments were performed in HBS-EP buffer, and regeneration of the anti-HIS surface was achieved with 20 mM HCl.

Equilibrium binding data for β2m was obtained by averaging a 5−10 s interval of normalized signal after reaching equilibrium. The equlibrium binding data were analyzed by nonlinear curve fitting of the Langmuir isotherm to the data or by linear fitting of a Scatchard plot. Dissociation data was analyzed by 1:1 Langmuir dissociation curve fitting. The curve fitting was performed using the BIAevaluation 3.0 software (Biacore AB). Data were normalized by subtracting the signal for a control surface prior to modeling. Equilibrium and dissociation constants of human and murine β2m at different temperatures were compared using the Student's *t* test. When multiple comparisons were made, the total *p* value of all significant comparisons was below 0.05. For thermodynamic analysis, ΔG was calculated from $-RT \ln K_a$, where R is the gas constant, T is the temperature in kelvin (K), and K_a is the equilibrium association constant. ΔH and ΔS were calculated from slope and intercept of the van't Hoff equation:

$$\ln K_a = -\Delta H/RT + \Delta S/R$$

ΔH and ΔS were also calculated using KaleidaGraph (Synergy Software, Reading, PA) to curve fit a nonlinear equation which takes into account the temperature dependence of ΔH and ΔS (*36*):

$$\Delta G^\circ_T = \Delta H_{T0} - T\Delta S^\circ_{T0} + \Delta C_p(T - T_0) + T\Delta C_p \ln(T/T_0)$$

where T is the temperature in kelvin (K), T_0 is an arbitrary reference temperature (298 K), ΔG°_T is the standard free energy of binding (kJ mol^{-1}) at T and is calculated from the equilibrium constant at temperature T, ΔH_{T0} is the enthalpy change (kJ mol^{-1}) upon binding at T_0, ΔS°_{T0} is the standard state entropy change (kJ mol^{-1}) upon binding at T_0, and ΔC_p is the specific heat capacity (kJ mol^{-1} K^{-1}) and is assumed to be temperature independent. The ΔG error was assessed by the SD of determinations from equilibrium binding experiments. The error of ΔH and ΔS was assessed through the curve fit. In evaluation of the equlibrium constants at differing temperatures, 25 °C (298 K) experiments were generally performed in the same runs to account for non-temperature-dependent variation. The calculated ΔC_p was close to zero (0.2 ± 0.8 kJ mol^{-1} K^{-1}) as expected from similar values of ΔH and ΔS seen with linear and nonlinear fits.

Analytical Ultracentrifugation. Analytical ultracentrifugation was carried out using a Beckman-Coulter (Fullerton, CA) XL-A centrifuge. An eight-place rotor was used with carbon-filled double-sector centerpieces in the cells. Two of the cells were loaded with different concentrations of SEC-purified α3 domain; two were loaded with different concentrations of SEC-purified hβ2m; three were loaded with mixtures of different molar ratios of α3 and hβ2m with total concentrations comparable to those in the other cells. Solution column heights were approximately 5 mm. Rotor speed was 17 000 rpm at an initial temperature of 5 °C because of the time required to attain equilibrium, which was 68 h. The temperature was then raised to 25 °C, but it was found that some of the gradients were not stable at that temperature, probably as a result of the samples being at the higher temperature for 48 h. Thus, only 5 °C results will be presented here.

Data analysis was performed by mathematical modeling using MLAB (Civilized Software, Silver Spring, MD) to fit the data by weighted nonlinear least-squares curve fitting to appropriate models (*37*). The reactants could be fit with a model for a thermodynamically ideal monomeric solute using the function:

$$A_r = A_b \exp(A'M'(r^2 - r_b^2)) + \epsilon$$

where A_r is the absorbance at 280 nm as a function of radial position; A_b is the absorbance at the radial position of the cell bottom r_b and is a fitting parameter; $A' = \omega^2/2RT$, where ω is the rotor angular velocity in radians per second, R is the gas constant, and T is the absolute temperature; M', which

is a fitting parameter, is the reduced molar mass and is equal to $M(1 - \bar{v}\rho)$, where M is the anhydrous molar mass, $\bar{v}$ is the partial specific volume, and ρ is the solvent density; and ϵ is a small baseline error term. The use of this function not only permits assessment of the monomeric state of a component but also experimentally determines the value of the reduced mass of the component in the model for the interaction. For monomeric reactants, this approach is optimal because it eliminates the need of either measuring partial specific volumes or computing them from the amino acid composition and also gives an optimal experimentally determined value for the reduced molar mass. Accordingly, this model was used for globally fitting both of the two appropriate data sets for each component, where M' was a global parameter and the other fitting parameters were local to each data set. Weight vectors were generated using the EWT function of MLAB. This is done by nonparametrically fitting each data set by multiple smoothing and, by squaring the deviation of each point, obtaining its variance; the individual weight is then the reciprocal of the variance. To obtain meaningful values for the root-mean-square (RMS) error, it is necessary to normalize each weight to unity by multiplying it by the number of values in the weighting vector and dividing this by the sum of the weights in the vector. In effect, this gives a mean value of one for the weights in the vector.

The association constant for the interaction was obtained by using a model for a one-to-one stoichiometry of association and performing global weighted fits to three data sets where the reactants were present in different molar ratios, these being approximately 1:1, 1:2, and 2:1. This model is given by

$$A_r = A_{b,1}\exp(A'M'_1(r^2 - r_b^2)) + A_{b,2}\exp(A'M'_2(r^2 - r_b^2)) + A_{b,1}A_{b,2}\exp(\ln K - \ln E + A'(M'_1 + M'_2)(r^2 - r_b^2)) + \epsilon$$

The A_b's are the absorbances for the respective components, the $A'M'$s are the reduced masses, ln K is the natural logarithm of the molar equilibrium constant, and ln $E = \ln(E_1E_2/(E_1 + E_2))$, where the E's are the molar extinction coefficients of the components at 280 nm. This term is necessary to convert ln K from a molar scale to an absorbance scale. The fitting parameters are then the global value of ln K and the local values of the A's and the ϵ's. We fit for ln K because this prevents obtaining negative, physically nonmeaningful values for K, and also, because $\Delta G^\circ = -RT \ln K$, we obtain a value with an appropriate error that reflects the change in standard free energy.

RESULTS

β2m-Driven Folding of Cell Surface MHC1 Heavy Chain. To study the species specificity of the β2m interaction with isolated α3 domains, we expressed human and murine β2m proteins using constructs in bacterial expression vectors (*32*, *33*). To assess the ability of these β2m molecules to fold MHC1 heavy chain, they were added to a peptide transport deficient cell line, LKD8 (*34*). This cell line lacks stable folded H-2D^d heavy chain as demonstrated by poor binding of the conformational epitope dependent anti-H-2D^d antibody, 34.5.8S. Addition of increasing amounts of either human or murine β2m to these cells, with an overnight incubation at 26−28 °C, leads to increasing amounts of folded cell surface H-2D^d MHC1 (Figure 1A). The increase in folded MHC1, shown by the increased binding of 34.5.8S, is greater with the addition of human β2m than with the addition of murine β2m (Figure 1B). This confirms previous findings that human β2m is more effective than murine β2m in generating folded MHC1 on the surface of peptide transport deficient cell lines (*28*, *32*). Our data, as well as previously published data (*20*, *21*, *28*), confirms that with both species of β2m the increase in folded MHC1 occurs at micromolar concentrations, not the nanomolar concentrations expected from β2m binding to MHC1 (*24*−*27*).

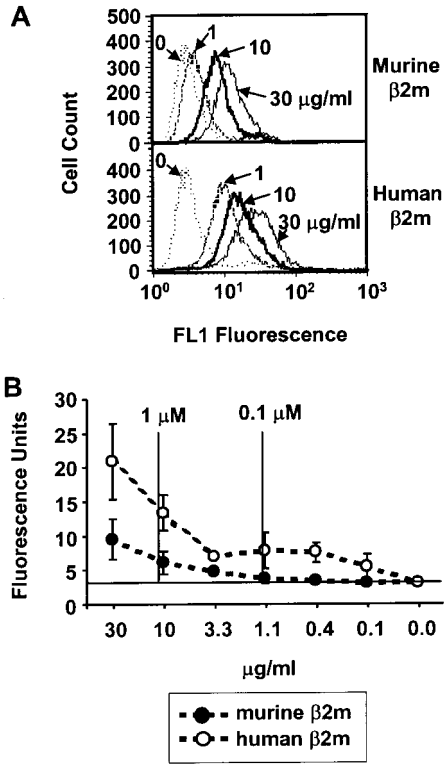

FIGURE 1: Human β2m is more effective than murine β2m in refolding of cell surface H-2D^d. Human or murine β2m was added overnight at the indicated concentrations to the peptide transport deficient cell line LKD8, and the folding of MHC1 was assessed by evaluating LKD8 staining with a conformationally dependent antibody to H-2D^d MHC1, 34.5.8S. (A) The staining of the LKD8 cells by biotin-labeled 34.5.8S followed by FITC−streptavidin is increased as the concentration of human or murine β2m is increased. Histograms of cells incubated with 0 (···), 1 (---), 10 (—), and 30 (—) μg of β2m are shown. (B) The median fluorescence of 34.5.8S staining LKD8 cells is increased to a greater extent by human β2m (○) than by murine β2m (●). The average and range of two experiments are shown. Controls with FITC−streptavidin alone had median fluorescence of 2−3 units.

Previous studies have demonstrated that the folding of MHC1 by β2m, in the absence of added MHC1 binding peptide, is much more efficient at room temperature than at 37 °C (*20*, *21*, *38*). This low-temperature induced expression of folded MHC1 in peptide transport deficient cells is dependent on the presence of β2m. MHC1 molecules expressed in this manner contain very few detectable peptides, as determined by peptide elution and HPLC analysis (*39*). One possible cause of the low-temperature enhancement of β2m-induced MHC1 expression is temperature effects on

protein transport to the cell surface. This cannot be the only cause for the temperature dependence since β2m induced MHC1 at 25−26 °C becomes unstable at 37 °C (*21*, *38*). This occurs in the presence of brefeldin A, so differential protein transport is not a factor in the reduced MHC1 expression. In addition, the folding of MHC1 at 4 °C by β2m in cell lysates, in which protein transport is not an issue (*22*, *23*), supports β2m as a critical factor in low-temperature folding of MHC1. Thus, a model for the mechanism of β2m folding of MHC1 should account for the micromolar concentration, species, and temperature dependence observed.

Monomeric α3 Domains Bind β2m with a 1:1 Stoichiometry. To evaluate β2m binding to isolated α3 domains, we needed to verify that such binding could be modeled by a 1:1 Langmuir binding isotherm ($A + B \Leftrightarrow AB$). Size exlusion chromatography (SEC) of the β2m molecules shows a monomer-sized peak which is purified shortly prior to binding experiments (data not shown). However, the α3 domain protein preparations have two size peaks upon SEC (Figure 2A), a predominant peak at approximately 24 kDa and a minor peak at 67 kDa. To confirm that the major peaks of the α3 and β2m proteins are monomeric, we performed analytical ultracentrifugation as per the Experimental Procedures. Using this approach, the reduced molar masses were found to be 4377 ± 40 and 3462 ± 121 for the α3 domain and human β2m, respectively. The weighted RMS errors were 0.0046 and 0.0045 absorbance unit. These reduced masses gave calculated values of 0.2925 and 0.2947 for $(1 - \bar{\nu}\rho)$ for the two proteins. These correspond to an approximate value of 0.7 for the partial specific volumes, which is somewhat lower than the values of 0.736 and 0.738 for the respective proteins calculated from their amino acid composition. This difference cannot be attributed to any degree of dimerization of either of the proteins since the quality of the joint fits of a monomeric model to data from significantly different loading concentrations precludes this possibility. Thus, it can be asserted that both proteins are demonstrably monomeric.

To evaluate the binding of β2m to the α3 domain protein, a biosensor for SPR was used. Antibody to the polyhistidine tail of the α3 proteins was directly coupled to the carboxymethylated dextran surface of a biosensor chip, allowing for the capture of α3 proteins on this surface. Murine β2m (mβ2m) was injected across the surface of immobilized α3 protein, and the binding was assessed by mass-related changes in the sensor chip matrix refractive index and quantified as response units (RU). β2m was also injected across a control surface consisting of the directly coupled capture antibody without α3 protein. This allowed protein concentration effects on the refractive index response to be subtracted out. An example of such an experiment is shown in Figure 2B. The responses of the α3 domain and control surfaces were normalized to each other immediately prior to the injection of the β2m to allow comparison of the active and control surfaces in this figure. Increasing concentrations of mβ2m were then evaluated for binding to either purified monomeric or multimeric α3 domains. The binding curves after subtraction of the control surface are shown in Figure 2C. It is clear that the multimer of α3 is unable to bind β2m at the concentrations evaluated, and the α3 monomer is responsible for α3 binding of β2m. This was also observed in experiments with human β2m (hβ2m; data not shown).

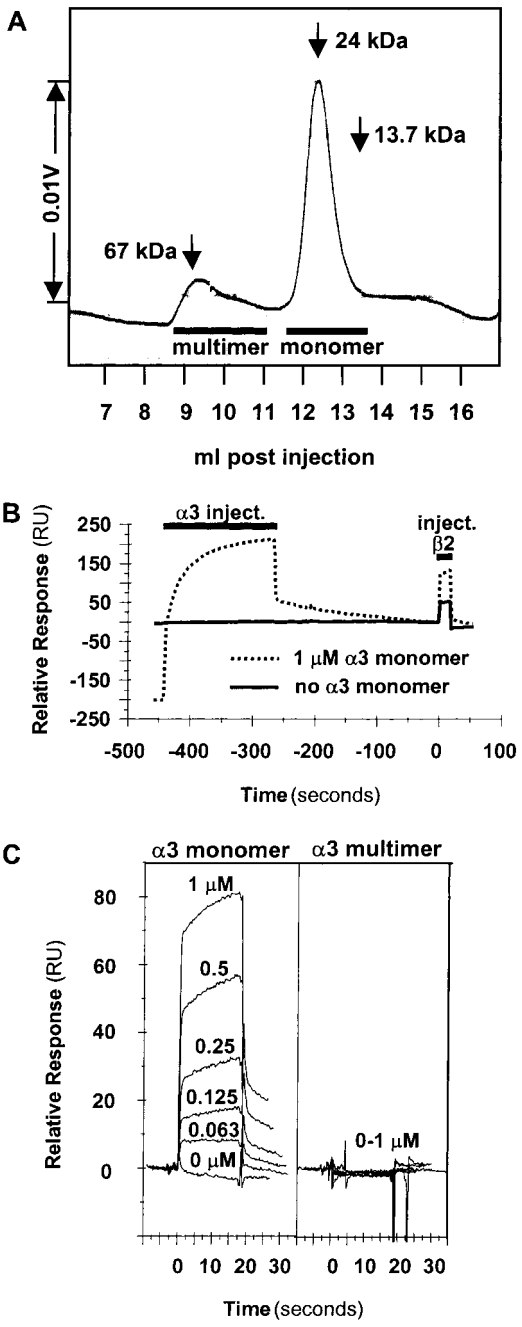

FIGURE 2: Measurement of β2m binding to the H-2D^d α3 domain. (A) 10 μg of α3 domain protein was injected on a Superdex 75 size exclusion chromatography column and eluted at 0.5 mL/min with HBS-EP buffer. The protein elution profile at 280 nm absorption is shown with the elution volumes of the standards BSA, trysinogen, and RNase. Monomeric and multimeric areas of the elution profile are indicated. (B) Anti-polyhistidine antibody was immobilized on two surfaces of an SPR sensor chip at 13 100 and 14 600 RU by amide coupling. 1 μM α3 domain (···) was injected over the 13 100 RU anti-polyhistidine surface, and buffer (—) was injected over the 14 600 RU anti-polyhistidine surface for 3 min at a flow rate of 10 μL/min. After a 4.5 min wait, 1 μM mβ2m was injected over both surfaces for 20 s at a flow rate of 30 μL/min. The responses of the two surfaces were normalized prior to the β2m injection to allow comparison of the β2m binding to α3 par and the control surface without α3 protein. (C) The response of the control surface to mβ2m was subtracted from the response of the α3 surface to mβ2m as a measure of β2m−α3 binding. Binding is shown for β2m to surfaces of purified α3 monomer and purified α3 multimer. The binding curves shown are at the indicated concentrations of mβ2m. Similar results were obtained for comparative binding of hβ2m to α3 monomer and α3 multimer surfaces.

To evaluate the nature of β2m binding to monomeric α3, we established the stoichiometry of the binding. The addition of an excess of β2m (8 μM) to immobilized α3 and evaluation of the bound RU demonstrated one β2m per α3 domain. Excess hβ2m led to 102% ± 3% of the expected binding for a 1:1 interaction with the α3 domain, and excess mβ2m led to 97% ± 0.7% of the expected binding for a 1:1 interaction with the α3 domain. To rule out negative or positive cooperativity between the immobilized α3 domains upon the binding of β2m, we evaluated the dependence of β2m dissociation on the contact time of β2m with the α3 domain surface. If the immobilized α3 domains were not independent in binding β2m, the increase in contact time would lead to a change in the dissociation curve (*40*), and such a change with contact time was not observed (data not shown).

To confirm the α3−β2m binding with an alternate method, we used analytical ultracentrifugation as described in Experimental Procedures. The global weighted fit of three data sets, with reactants at molar ratios of 1:1, 1:2, and 2:1, gave a value for ln K of 12.47 ± 0.16, which gives a value for $\Delta G°$ of −28.8 ± 0.38 kJ/mol (−6.89 ± 0.09 kcal/mol) at 5 °C and a value of 3.86 ± 0.62 μM for the equilibrium dissociation constant. The joint fit had a weighted RMS error of 0.0038 absorbance unit, clearly indicating that the one-to-one stoichiometry was the correct model for the association. The equilibrium dissociation constant, although higher than that measured using the Biacore, is still in the micromolar range. Biacore measurements of the interaction immobilizing β2m also gave a somewhat higher dissociation constant that that of the interaction with immobilized α3 (data not shown). The α3 peptide extension and polyhistidine tail may interfere with the binding and are sequestered when a3 is immobilized through antibody to the polyhistidine tail.

Our data demonstrate that the α3 domain exists as a monomer, it binds β2m with a 1:1 stoichiometry, and this binding shows no evidence of cooperativity. The β2m interaction with the α3 domain can be modeled by 1:1 Langmuir binding and occurs with a dissociation in the micromolar range.

β2m Equilibrium Binding to the α3 Domain. Human and murine β2-microglobulin were used to evaluate the binding parameters of β2m to the MHC1 α3 domain. Whole murine MHC class I binds human β2m with a K_d of 4×10^{-10} M (*27*) and murine β2m with a 3-fold lower affinity (*41*). We evaluated β2m binding by comparing α3 parental (α3 par) and control surfaces as shown in Figure 2B and taking equilibrium values of the subtracted data as shown in Figure 2C. The equilibrium values were used to generate the plots in Figure 3, which were used for equilibrium fitting. Figure 3A shows nonlinear curve fits of the Langmuir isotherm for murine and human β2m binding to the α3 domain. The same data are graphed as Scatchard plots in Figure 3B. The linearity of the Scatchard plots confirms the lack of cooperativity in the binding.

The equilibrium constants generated from three experiments with each of the β2m proteins are shown in Table 1. Human β2m binds isolated α3 domains with an equilibrium K_d of 3.4×10^{-7} M, which is 2-fold better than murine β2m. This advantage of human β2m remains when the α3 CD loop is mutated at position 227 with concurrent loss of CD8 binding (*29*). The superior binding of human β2m to isolated

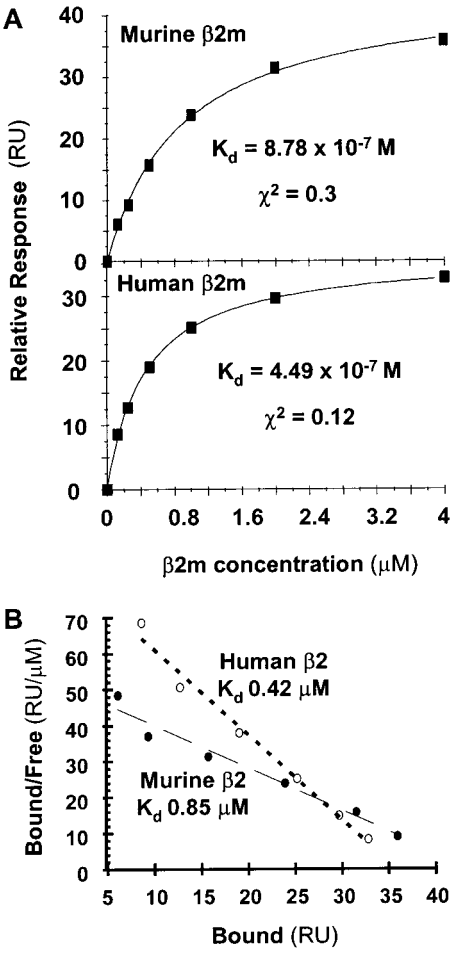

FIGURE 3: Human β2m has a higher affinity for the α3 domain than murine β2m. (A) Averages of the equilibrium β2m−α3 binding responses during β2m injection were plotted versus β2m concentration. These points were fit with the Langmuir isotherm to determine the K_d. The χ^2 (average of the squared residuals) values of 0.3 and 0.12 suggest good fits. (B) The same equilibrium binding data for human (○) and murine (●) β2m is shown transformed into a Scatchard plot. The K_d was determined from the negative inverse of the slope of the fitted line.

α3 domains correlates with the superior MHC1 folding ability previously shown. In Table 1 we also evaluate the effect of temperature on β2m binding to the α3 domain. The affinity of both human and murine β2m is decreased 3-fold by raising the assay temperature from 25 to 37 °C. The improved β2m binding to the α3 domain at room temperature correlates with the superior β2m-driven refolding of MHC1 at room temperature (*20*, *21*, *38*). It is of note that the difference in binding between human and murine β2m to α3 domains is only 2-fold while human β2m has been reported to be 4−20 times more effective at folding MHC1 heavy chain than murine β2m (*28*). One possible explanation for this difference is that hβ2m has an advantage in refolding α1α2 domains in addition to binding the α3 domain. The MHC1 refolding advantage of hβ2m was reduced by mutation of a β2m residue which contacts the α1α2 domains of MHC1 (*32*). Since mutations in the α1α2 interface of β2m have variable effects on the folding of different MHC1 haplotypes, this interface may also contribute to the larger overall advantage of human versus murine β2m.

There is another factor that could explain the difference between relative α3 binding and relative MHC1 refolding

Table 1: Equilibrium Binding of β2m to MHC1 α3 Domain Proteins[a]

		25 °C		37 °C	
β2m protein	α3 protein	K_d (M)	χ^2	K_d (M)	χ^2
murine	α3 par	$6.9 \pm 1.7 \times 10^{-7}$	0.29 ± 0.21	$2.1 \pm 0.27 \times 10^{-6}$	0.18 ± 0.11
murine	α3 227m	$6.0 \pm 1.3 \times 10^{-7}$	0.13 ± 0.03	not performed	
human	α3 par	$3.4 \pm 1.1 \times 10^{-7}$	0.11 ± 0.04	$1.1 \pm 0.19 \times 10^{-6}$	0.09 ± 0.05
human	α3 227m	$3.9 \pm 0.3 \times 10^{-7}$	0.14 ± 0.07	not performed	

[a] The equilibrium fit was determined from a nonlinear Langmuir isotherm fit of equilibrium data similar to that of Figure 3A. The fitting was done using the Biaevaluation 3.0 software as per the Experimental Procedures. The K_d results are the average of three experiments ± the standard deviation. The χ^2 average ± the standard deviation is shown as a measure of the curve fit. The K_d of both β2m are significantly different from each other ($p < 0.045$). The K_d at 37 °C is significantly different from the K_d at 25 °C ($p < 0.002$).

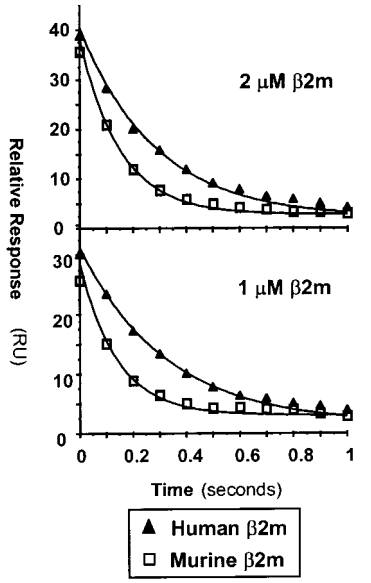

FIGURE 4: Human β2m dissociates more slowly from the α3 domain than murine β2m. The dissociation of human (▲) and murine (□) β2m from α3 is shown after the injection of 1 or 2 μM β2m. The curves are 1:1 Langmuir fits of the dissociation data used in determining the dissociation constants shown in Table 2.

of the different β2m species. After β2m binding of the MHC1 α3 domain, a discrete interval of time may be required for potential multiple steps in the β2m folding of the α1α2 domains of the MHC1 heavy chain. If this is the case, the association of β2m with the MHC1 α3 domain may be a kinetic intermediate, and a 2-fold change in half-life of that intermediate may have greater than a 2-fold effect on the yield of folded MHC1. This greater effect would operate through a mechanism similar to kinetic proofreading (*42*). The shorter murine β2m dwell time would decrease the probability of an initial step in α1α folding that would slow the β2m dissociation. This would then lead to an even lower probability of completion of α1α2 domain folding than the difference in β2m−α3 half-life. To explore this possibility, we evaluated the dissociation kinetics of human and murine β2m binding to the α3 domain.

Human β2m Bound to the α3 Domain Has a 2-fold Longer Half-Life Than Murine β2m. To evaluate the dissociation of the β2m from the α3 domain of MHC1, α3 was immobilized on a sensor chip by capture with anti-HIS antibody, and β2m binding was evaluated as described above. Because of the rapidity of the dissociation, data points were captured at 0.1 s intervals and a high flow rate of 30 μL/min was used for the β2m injection. Figure 4 shows the dissociation phase of the β2m−α3 interaction and demonstrates that human β2m dissociates more slowly than murine β2m. Table 2 shows

Table 2: Dissociation of Human and Murine β2m from MHC1 α3 Domain Protein[a]

β2m concn (μM)	k_{off} (s^{-1})	
	human β2m	murine β2m
4	2.42	3.18
2.5	2.48	5.78
2	1.49	4.30
1.25	2.72	4.27
1	1.54	4.01
0.625	2.45	4.17
av ± SD	2.18 ± 0.53	4.29 ± 0.84

[a] The dissociation constants (k_{off}s) were determined from a nonlinear Langmuir isotherm fit of dissociation data similar to that of Figure 4. The fitting was done using the Biaevaluation 3.0 software as per the Experimental Procedures. The k_{off} results at different concentrations of β2m were averaged, and the standard deviation is shown. The average χ^2 for the hβ2m fits was 0.2 and for the mβ2m fits was 0.69. The dissociation constants for human and murine β2m are significantly different from each other ($p < 0.01$).

the dissociation constants of human and murine β2m at a number of concentrations. No concentration dependence is evident, and the off rate of human β2m is one-half that of murine β2m. If the binding of β2m to the α3 domain of MHC1 is a kinetic intermediate in the β2m folding of MHC1, then the 2-fold longer dwell time of human β2m could account for an even greater effect on MHC1 folding.

β2m Binding to the α3 Domain Is Associated with Decreased Entropy. The temperature dependence of β2m refolding of cell surface MHC1 and binding to the MHC1 α3 domain is suggestive of an enthalpic-driven process in which entropy decreases upon binding. To better define the thermodynamic parameters of β2m−α3 binding, we evaluated the equilibrium binding of murine β2m to α3 at a number of different temperatures. We evaluated these SPR data as described by Roos et al. (*43*) using both a linear and nonlinear van't Hoff analysis. Figure 5A shows the plot of the linear analysis and the values of ΔH obtained from the slope and $-T\Delta S$ derived from ΔH and ΔG. The nonlinear analysis leads to very similar results with a ΔG of −35.2, a ΔH of −70.7, and a $-T\Delta S$ of 35.6 kJ/mol at 25 °C. In both cases $-T\Delta S$ has a positive value, suggesting a reduction of disorder during β2m−α3 binding. This is an unusual binding thermodynamics as shown by comparing the values to those of 30 nonantibody protein−protein interactions (*44*) (Figure 5B). Binding with decreasing disorder can be seen with TCR−MHC−peptide interactions and some antibody−antigen interactions (*45*, *46*).

DISCUSSION

β2m is both a structural component of MHC1 and a chaperone for correct folding of the MHC1 heavy chain. β2m

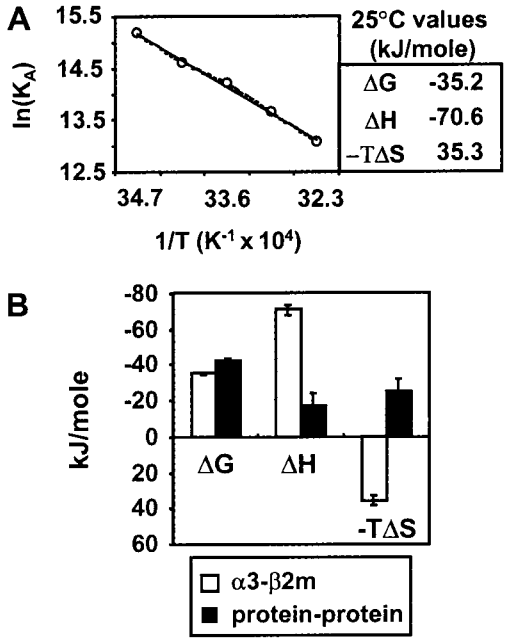

FIGURE 5: β2m binding to the α3 domain has an unfavorable entropy. (A) The equlibrium association binding constant (K_A) of mβ2m to α3 was determined at the temperatures 15, 20, 25, 30, and 37 °C (two to eight evaluations per temperature). The natural logarithm of the K_A was graphed against the inverse of temperature using the van't Hoff equation. The values of ΔH were obtained from the slope of the line, and $-T\Delta S$ was derived from ΔH and ΔG. (B) The thermodynamic parameters determined from the nonlinear van't Hoff relationship for β2m−α3 binding (□) were compared to those of a series of 30 nonantibody protein−protein interactions (■). The error bars for β2m−α3 binding are based on the SD of measured values or the error of curve fitting as per the Experimental Procedures. The error bars for the protein−protein interactions are the SEM of reported values.

binds folded MHC1 heavy chain at a 1000-fold lower concentration than that required for β2m refolding of cell surface MHC1. The α3 domain of the MHC1 heavy chain is folded before the other MHC1 domains prior to associating with β2m (*30*, *31*) and remains folded longest on the cell surface (*21*). This makes a β2m interaction with the α3 domain of heavy chain an attractive model for the β2m refolding of MHC1 heavy chain. We have previously demonstrated that human β2m binding to an isolated α3 domain has a micromolar affinity (*29*) similar to the concentration that β2m refolds MHC1. To provide further evidence that β2m refolds MHC1 by binding the α3 domain, we demonstrated that the α3 domain binds murine β2m in addition to binding human β2m. The binding of the α3 domain by β2m has a species hierarchy similar to the refolding of the MHC1 heavy chain. This β2m species difference in affinity is due to a difference in off rates and may be important in determining the half-life of a kinetic intermediate in MHC1 folding. We have also demonstrated that the β2m−α3 interaction has the same unusual temperature dependence as β2m-induced refolding of MHC1. These data strongly support a model in which a β2m−α3 interaction facilitates the folding of the MHC1 heavy chain.

A crystal structure of β2m binding the α1α2 domains of MHC1 (*47*) suggests that β2m can bind MHC1 in the absence of the α3 domain. It is of note that the MHC1 α3 domain was present during the refolding in this study and was only lost due to proteolysis during crystallization. MHC1 without the α3 domain can be expressed on cells and folded by large amounts of high-affinity peptide; however, the α3-deleted MHC1 is unable to be folded by β2m at any tested concentration (*23*). Therefore, neither of these studies demonstrates β2m-driven MHC folding without the α3 domain.

The temperature dependence of the β2m−α3 interaction led us to evaluate the thermodynamics of the interaction. We found that the binding is driven by a large enthalpy contribution which overcomes an unfavorable entropy of binding. This type of binding is generally not seen in protein−protein interactions which have coevolved to favor binding. Recently, binding which decreases disorder has been seen in T-cell receptor (TCR) interactions with peptide−MHC ligand (*45*, *46*). TCR does not necessarily coevolve with potential antigenic peptides, and the basic TCR structure must recognize a wide range of peptide−MHC complexes. The cross-reactivity of TCR recognition supports a model in which a flexible TCR can scan through a number of conformations until it optimizes interaction with a specific ligand interaction. The limitation of this flexibility upon binding the ligand increases order and exacts an entropic penalty on the overall binding affinity. Although the relatively nonpolymorphic β2m must interact with a wide variety of polymorphic MHC1 chains, β2m has coevolved with MHC1, and MHC1 polymorphisms tend to involve the peptide and TCR contacts. Scanning through a series of conformations is unlikely to be the cause of the increased order observed in the β2m−α3 interaction. β2m can fold the complete MHC1 heavy chain, and one previous study suggested that there is an entropic penalty for β2m exchange with whole MHC1 (*25*). The increased order involved in folding MHC1 could account for an unfavorable entropy of binding. This folding may also involve conformational changes in the α3 domain or β2m and account for our observed binding thermodynamics. Modeling of β2m interactions with MHC1 heavy chains suggests a conformational change of mβ2m upon binding (*48*). In addition, although we have been unable to accurately model the association constant in our antibody capture binding system, a number of experiments suggest an association constant of 10^6 M^{-1} s^{-1}, which is similar to the association constant calculated from the observed equilibrium and dissociation constants. This rapid on rate is different than the slow on rates seen with the TCR interactions and suggests that the entropic penalty seen during the β2m−α3 interaction is due to a defined conformational shift or ordering of water molecules rather than the time-consuming scanning of multiple conformations. Another example of binding with an increase in order is seen with Z, a one-domain analogue of protein A (*43*). This binding also has a rapid association constant in the range of 10^6 M^{-1} s^{-1}. This binding may also require a defined conformational change upon binding.

The binding and thermodynamic parameters of β2m interactions play an important role in MHC1 assembly in the ER. The β2m interaction with the α3 domain can be further evaluated with other fragments of the MHC1 heavy chain and whole MHC1 using SPR. The addition of MHC binding peptides and chaperone molecules such as calreticulin, tapasin, TAP, and Erp57 may allow for the understanding of the energetics of physiologic MHC1 folding in the ER.

The refolding of the free MHC1 heavy chain on the surface of cells by β2m plays an important role in normal cells (*49*−*51*) as well as peptide transport deficient cells. This refolding can have immunologic consequences due to the enhanced presentation of exogenous peptide fragments to CTL (*52*−*55*). Such presentation of extracellularly processed (*56*−*59*) class I restricted peptides could cause lysis of uninfected bystander cells in a CTL response to virus. Understanding the mechanism of MHC1 refolding may suggest strategies to prevent such aberrant responses.

The binding of the MHC1 heavy chain to β2m involves multiple domains with multiple contacts. We have analyzed the binding of isolated MHC1 α3 domains to β2m using SPR and obtained information important for understanding the mechanism of MHC1 folding. The analysis of the binding characteristics of individual domains and surfaces of complex biologic molecules is an important tool in elucidating the structural and functional behavior of these molecules.

ACKNOWLEDGMENT

We thank Drs. Sean Fitzsimmons, David H. Margulies, and Kathryn E. Stein for valuable discussion and support of this work.

REFERENCES

1. Townsend, A., and Bodmer, H. (1989) *Annu. Rev. Immunol. 7*, 601−624.
2. Jones, E. Y., Tormo, J., Reid, S. W., and Stuart, D. I. (1998) *Immunol. Rev. 163*, 121−128.
3. Germain, R. N., and Margulies, D. H. (1993) *Annu. Rev. Immunol. 11*, 403−450.
4. Ljunggren, H. G., and Thorpe, C. J. (1996) *Histol. Histopathol. 11*, 267−274.
5. Ozato, K., Evans, G. A., Shykind, B., Margulies, D. H., and Seidman, J. G. (1983) *Proc. Natl. Acad. Sci. U.S.A. 80*, 2040−2043.
6. Bjorkman, P. J., Saper, M. A., Samraoui, B., Bennett, W. S., Strominger, J. L., and Wiley, D. C. (1987) *Nature 329*, 512−518.
7. Davis, M. M., Boniface, J. J., Reich, Z., Lyons, D., Hampl, J., Arden, B., and Chien, Y. (1998) *Annu. Rev. Immunol. 16*, 523−544.
8. Saper, M. A., Bjorkman, P. J., and Wiley, D. C. (1991) *J. Mol. Biol. 219*, 277−319.
9. Santos-Aguado, J., Biro, P. A., Fuhrmann, U., Strominger, J. L., and Barbosa, J. A. (1987) *Mol. Cell. Biol. 7*, 982−990.
10. Ribaudo, R. K., and Margulies, D. H. (1995) *J. Immunol. 155*, 3481−3493.
11. Salter, R. D. (1992) *Hum. Immunol. 35*, 40−49.
12. Seong, R. H., Clayberger, C. A., Krensky, A. M., and Parnes, J. R. (1988) *J. Exp. Med. 167*, 288−299.
13. Zijlstra, M., Bix, M., Simister, N. E., Loring, J. M., Raulet, D. H., and Jaenisch, R. (1990) *Nature 344*, 742−746.
14. Allen, H., Fraser, J., Flyer, D., Calvin, S., and Flavell, R. (1986) *Proc. Natl. Acad. Sci. U.S.A. 83*, 7447−7451.
15. Bix, M., and Raulet, D. (1992) *J. Exp. Med. 176*, 829−834.
16. Solheim, J. C., Johnson, N. A., Carreno, B. M., Lie, W. R., and Hansen, T. H. (1995) *Eur. J. Immunol. 25*, 3011−3016.
17. Fink, A. L. (1999) *Physiol. Rev. 79*, 425−449.
18. Solheim, J. C. (1999) *Immunol. Rev. 172*, 11−19.
19. Cresswell, P., Bangia, N., Dick, T., and Diedrich, G. (1999) *Immunol. Rev. 172*, 21−28.
20. Rock, K. L., Gramm, C., and Benacerraf, B. (1991) *Proc. Natl. Acad. Sci. U.S.A. 88*, 4200−4204.
21. Otten, G. R., Bikoff, E., Ribaudo, R. K., Kozlowski, S., Margulies, D. H., and Germain, R. N. (1992) *J. Immunol. 148*, 3723−3732.
22. Elliott, T., Cerundolo, V., Elvin, J., and Townsend, A. (1991) *Nature 351*, 402−406.
23. Elliott, T., Elvin, J., Cerundolo, V., Allen, H., and Townsend, A. (1992) *Eur. J. Immunol. 22*, 2085−2091.
24. Hyafil, F., and Strominger, J. L. (1979) *Proc. Natl. Acad. Sci. U.S.A. 76*, 5834−5838.
25. Parker, K. C., and Strominger, J. L. (1985) *Biochemistry 24*, 5543−5550.
26. Hochman, J. H., Shimizu, Y., DeMars, R., and Edidin, M. (1988) *J. Immunol. 140*, 2322−2329.
27. Pedersen, L. O., Hansen, A. S., Olsen, A. C., Gerwien, J., Nissen, M. H., and Buus, S. (1994) *Scand. J. Immunol. 39*, 64−72.
28. Shields, M. J., Moffat, L. E., and Ribaudo, R. K. (1998) *Mol. Immunol. 35*, 919−928.
29. Whitman, M. C., Strohmaier, J., O'Boyle, K., Tingem, J. M., Wilkinson, Y., Goldstein, J., Chen, T., Brorson, K., Brunswick, M., and Kozlowski, S. (2000) *Mol. Immunol. 37*, 141−149.
30. Elliott, T. (1991) *Immunol. Today 12*, 386−388.
31. Ribaudo, R. K., and Margulies, D. H. (1992) *J. Immunol. 149*, 2935−2944.
32. Shields, M. J., Assefi, N., Hodgson, W., Kim, E. J., and Ribaudo, R. K. (1998) *J. Immunol. 160*, 2297−2307.
33. Shields, M. J., Kubota, R., Hodgson, W., Jacobson, S., Biddison, W. E., and Ribaudo, R. K. (1998) *J. Biol. Chem. 273*, 28010−28018.
34. Bikoff, E. K., Otten, G. R., and Robertson, E. J. (1991) *Eur. J. Immunol. 21*, 1997−2004.
35. Johnsson, B., Lofas, S., and Lindquist, G. (1991) *Anal. Biochem. 198*, 268−277.
36. Naghibi, H., Tamura, A., and Sturtevant, J. M. (1995) *Proc. Natl. Acad. Sci. U.S.A. 92*, 5597−5599.
37. Lewis, M. S. (1996) in *Exploration 3*, pp 11−16, Beckman-Coulter.
38. Ljunggren, H. G., Stam, N. J., Ohlen, C., Neefjes, J. J., Hoglund, P., Heemels, M. T., Bastin, J., Schumacher, T. N., Townsend, A., Karre, K., et al. (1990) *Nature 346*, 476−480.
39. Anderson, K. S., Alexander, J., Wei, M., and Cresswell, P. (1993) *J. Immunol. 151*, 3407−3419.
40. Karlsson, R., and Falt, A. (1997) *J. Immunol. Methods 200*, 121−133.
41. Pedersen, L. O., Stryhn, A., Holter, T. L., Etzerodt, M., Gerwien, J., Nissen, M. H., Thogersen, H. C., and Buus, S. (1995) *Eur. J. Immunol. 25*, 1609−1616.
42. Hopefield, J. J. (1974) *Proc. Natl. Acad. Sci. U.S.A. 71*, 4135−4139.
43. Roos, H., Karlsson, R., Nilshans, H., and Persson, A. (1998) *J. Mol. Recognit. 11*, 204−210.
44. Stites, W. E. (1997) *Chem. Rev. 97*, 1233−1250.
45. Willcox, B. E., Gao, G. F., Wyer, J. R., Ladbury, J. E., Bell, J. I., Jakobsen, B. K., and van der Merwe, P. A. (1999) *Immunity 10*, 357−365.
46. Boniface, J. J., Reich, Z., Lyons, D. S., and Davis, M. M. (1999) *Proc. Natl. Acad. Sci. U.S.A. 96*, 11446−11451.
47. Collins, E. J., Garboczi, D. N., Karpusas, M. N., and Wiley, D. C. (1995) *Proc. Natl. Acad. Sci. U.S.A. 92*, 1218−1221.
48. Shields, M. J., Hodgson, W., and Ribaudo, R. K. (1999) *Mol. Immunol. 36*, 561−573.
49. Smith, M. H., and Barber, B. H. (1990) *Mol. Immunol. 27*, 169−180.
50. Rock, K. L., Gamble, S., Rothstein, L., Gramm, C., and Benacerraf, B. (1991) *Cell 65*, 611−620.
51. Smith, J. D., Lie, W. R., Gorka, J., Myers, N. B., and Hansen, T. H. (1992) *Proc. Natl. Acad. Sci. U.S.A. 89*, 7767−7771.
52. Vitiello, A., Potter, T. A., and Sherman, L. A. (1990) *Science 250*, 1423−1426.
53. Rock, K. L., Rothstein, L. E., Gamble, S. R., and Benacerraf, B. (1990) *Proc. Natl. Acad. Sci. U.S.A. 87*, 7517−7521.
54. Kozlowski, S., Takeshita, T., Boehncke, W. H., Takahashi, H., Boyd, L. F., Germain, R. N., Berzofsky, J. A., and Margulies, D. H. (1991) *Nature 349*, 74−77.

55. Kane, K. P., Sherman, L. A., and Mescher, M. F. (1991) *Eur. J. Immunol. 21*, 2289−2292.
56. Sherman, L. A., Burke, T. A., and Biggs, J. A. (1992) *J. Exp. Med. 175*, 1221−1226.
57. Kozlowski, S., Corr, M., Takeshita, T., Boyd, L. F., Pendleton, C. D., Germain, R. N., Berzofsky, J. A., and Margulies, D. H. (1992) *J. Exp. Med. 175*, 1417−1422.
58. Falo, L. D., Jr., Colarusso, L. J., Benacerraf, B., and Rock, K. L. (1992) *Proc. Natl. Acad. Sci. U.S.A. 89*, 8347−8350.
59. Kozlowski, S., Corr, M., Shirai, M., Boyd, L. F., Pendleton, C. D., Berzofsky, J. A., and Margulies, D. H. (1993) *J. Immunol. 151*, 4033−4044.

BI002392S